

Textured fluorine-doped ZnO films by atmospheric pressure chemical vapor deposition and their use in amorphous silicon solar cells

Jianhua Hu and Roy G. Gordon

Department of Chemistry, Harvard University, Cambridge, MA 02138 (U.S.A.)

(Received October 25, 1990)

Abstract

Fluorine-doped ZnO films were deposited on soda lime glass by atmospheric pressure chemical vapor deposition at temperatures from 350 to 470 °C by using diethyl zinc, ethanol and hexafluoropropene as precursors. The deposited films typically contained about 0.1 to about 1.0 at.% fluorine with conductivities up to $2500 \Omega^{-1} \text{ cm}^{-1}$. The free electron concentrations determined from Hall coefficient measurements were up to $5 \times 10^{20} \text{ cm}^{-3}$ and the mobilities were between 10 and $40 \text{ cm}^2 \text{ V}^{-1} \text{ s}^{-1}$. The films with very low sheet resistances of $5 \Omega/\square$ were found to have visible absorption of only 3% and transmittance up to 90% in the visible and reflectance of about 85% in the infrared. The film roughness was controlled by the deposition temperature and by introducing a small amount of water vapor. The rough films were used as substrates for amorphous silicon solar cells with very high quantum efficiency (up to 90%).

1. Introduction

ZnO films have numerous applications as window materials for solar cells, gas sensors, surface acoustic wave devices, ultrasonic transducers and ultrasonic oscillators because of their excellent electrical, optical and acoustic properties [1]. Pure ZnO is a semiconductor with an energy band gap of about 3.3 eV which has low electrical conductivity and low reflectance in the infrared. Films made to be non-stoichiometric or doped with foreign atoms such as fluorine [2], boron [3], aluminum and indium [4] have high conductivity. The non-stoichiometric films are the simplest and the most economical to prepare, and their electrical and optical properties are also excellent, but they are not very stable at high temperatures. Heat treatment of non-stoichiometric films at 400 °C can increase the sheet resistance by factors of 10 to 1000 [5]. On the other hand, the doped ZnO films can have more stable electrical properties.

It is important to choose the dopant which will give ZnO the highest conductivity and transparency. These properties will be highest for the dopant which produces the highest electron mobility. We now argue that fluorine will produce higher mobilities than the group III metals. Group III atoms

presumably become electrically active as n-type dopants in ZnO when they substitute for zinc atoms. In a relatively ionic semiconductor like ZnO, the conduction band derives mainly from the metal (zinc) orbitals. Thus every dopant metal atom represents a strong local perturbation to the conduction band, which causes strong scattering of the electrons in the conduction band, thereby reducing their mobility. On the other hand, dopants which substitute for oxygen, rather than zinc, would perturb mainly the valence band, leaving the conduction band relatively free of scattering, with a higher electron mobility. Halogen atoms substituting for oxygen would therefore be expected to be n-type dopants which retain high electron mobility. The heavier halogens, chlorine, bromine and iodine, are too large to substitute for oxygen without large distortions of the crystal lattice. However, fluorine ions are about the same size as oxide ions, and thus fluorine would be predicted to be an n-type dopant which maintains the highest electron mobility in ZnO. A second disadvantage of these group III elements is that they can also dope amorphous silicon (a-Si) films. Out-diffusion of these dopants from the doped ZnO into the a-Si can degrade the cell efficiency either during deposition or in use, and so it is desirable to find a dopant for ZnO which is not electrically active in a-Si. Fluorine, which is known to be electrically inactive, or even beneficial, in hydrogenated a-Si, satisfies these conditions and would therefore be an ideal dopant.

The deposition of ZnO films on various substrates has been achieved by techniques such as chemical vapor deposition (CVD), r.f. magnetron sputtering, reactive sputtering, vacuum evaporation and spray pyrolysis. Chemical vapor deposition is especially useful for large scale coating at high growth rates. The most commonly used organometallic zinc precursors are diethyl zinc (DEZ) [6] and dimethyl zinc (DMZ) [7]. Although DMZ can react with oxygen at atmospheric pressure to coat the substrate over a large area at a reasonable growth rate [8], it is more expensive and dangerous to handle. DEZ is much cheaper and has been widely used to deposit both pure and doped ZnO films. The reaction between DEZ and oxygen is difficult to control and premature reaction upstream can produce powder even at low concentrations of the reactants. The reaction of DEZ and alcohol depends on the alcohol used and the deposition temperature [9]. Uniform films can be produced at reasonably high growth rates by choosing different alcohols at different temperatures.

In this paper we report for the first time that highly conductive, fluorine-doped ZnO films have very low visible absorption, and can be textured to provide efficient light-trapping in a-Si solar cells. The textured, fluorine-doped films have been successfully deposited from diethyl zinc, ethyl alcohol, water vapor and hexafluoropropene. The films were characterized by ellipsometry, X-ray diffraction, scanning electron microscopy and electron microprobe analysis. The resistance and Hall coefficient measurements were used to find the film resistivities, electron concentrations and mobilities. Optical measurements showed the doped films with desired roughness had low absorption and high transmittance in the visible range and high reflectance in the infrared.

Solar cells made from the textured, fluorine-doped films had very high quantum efficiencies.

2. Experimental procedure

The ZnO deposition apparatus is shown schematically in Fig. 1. The nickel reactor has a special nozzle, designed by the Watkins—Johnson Company, with three separated gas inlet lines. This design is helpful in moderating the fast reaction of DEZ and ethanol at high temperatures. The inner line and the outer lines are used to introduce DEZ and ethanol vapor, respectively. The middle line is for buffer helium which keeps DEZ and ethanol separated for a small distance after being injected into the reactor. The reactor is a rectangular chamber 1 cm high, 12.5 cm wide and 30 cm long operating at one atmosphere pressure. Substrates rest on the bottom of this chamber. The reactor was placed on a hot plate, and the thermocouples for the temperature controller were inserted in holes in the bottom plate of the reactor. The deposition temperature can be stabilized to $\pm 1^\circ\text{C}$, and the deposition reaction of DEZ and ethanol was studied over the temperature range from 300°C to 470°C at atmospheric pressure. An oven was used to heat the alcohol bubbler to 60°C in order to achieve a high vapor pressure and the temperature of the DEZ bubbler was kept at 25°C throughout the

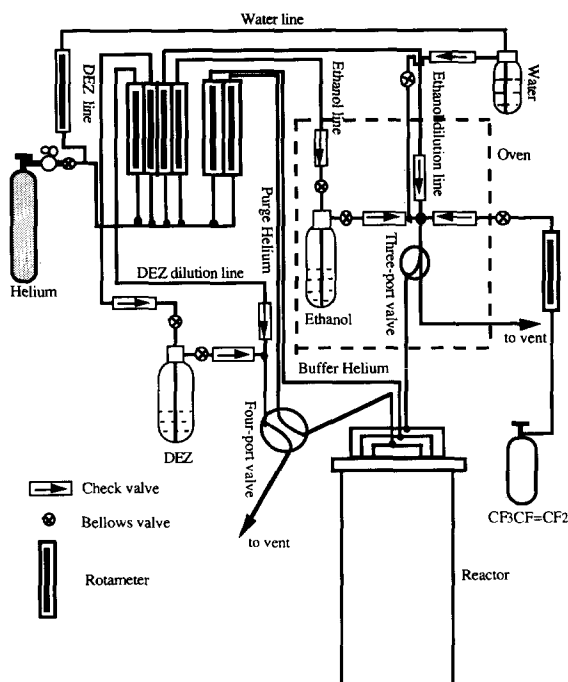


Fig. 1. Schematic diagram of the ZnO:F film deposition system.

experiments. The DEZ and alcohol vapors were carried by helium from their bubblers and then further diluted by pure helium from dilution lines. The gas flow for DEZ, ethanol and buffer lines were each 4.0 l min^{-1} and therefore the total gas flow was fixed at 12.0 l min^{-1} . The DEZ and alcohol concentrations in the gas mixture were calculated by assuming that the carrier helium was saturated in each bubbler. There are two other ports attached to the alcohol dilution line. One is used to introduce the fluorine dopant gas (hexafluoropropene from PCR, Inc.) and the other the water vapor. A four-port valve and a three-port valve controlled by an air-actuator and a timer were used to switch on and off the reactant gases.

Films less than 1500 \AA thick were measured with a Rudolph Research AutoEL-II ellipsometer to determine their thickness and refractive index. The best results were obtained for thicknesses above 500 \AA and below the full cycle thickness (usually about 1900 \AA for ZnO films with a refractive index of about 1.95). Thicknesses of thicker films were determined by fitting visible reflectance data and by using a Metricon PC-2000 prism coupler. X-ray diffraction measurements were made on a Philips powder crystallography instrument by using copper K_α radiation. A JEOL JSM-35 scanning electron microscope (SEM) was used to obtain the crystallite orientation and size. Film compositions were found by a Cameca MBX electron microprobe equipped with a Tracor Northern TN-5502 EDS system and a TN-1310 wavelength dispersive spectrometer. The standards used for zinc and fluorine were pure ZnO and CaF_2 . The oxygen concentration was not determined. Resistance and Hall coefficient measurements were made to find the electron concentrations and the mobilities of the doped films. The infrared spectra were taken on a Nicolet model 7199 Fourier transform spectrometer with a relative reflection attachment. A gold mirror with a known reflectance was used as the reflectance standard. Near ultraviolet, visible and near infrared spectra were obtained with a Varian 2390 spectrophotometer using an integrating sphere detector which could measure both total and diffuse components of the reflectance and transmittance. The absorption of light within a film was then found by subtracting the total reflectance and total transmission from 100%. For films with rough surfaces, however, this absorption value is unrealistically high because some light is trapped within the ZnO film and travels in the plane of the film until it is absorbed. In a solar cell containing both ZnO and a-Si layers, most of the light will be trapped in the silicon layer, since it has a higher refractive index than the ZnO. Therefore, to provide a better measure of light absorbed during one pass through the ZnO layer, spectra of rough ZnO films were obtained by covering the film surface with a thin layer of liquid with a high refractive index (1.74, from Cargille Industries, Inc.). The measured absorptions of the films were further corrected for absorption by the liquid, a cover glass and the glass substrate. The films with desired properties were used at Solarex, Inc. to prepare "standard" p a-SiC:H/i a-Si:H/n a-Si:H devices with indium tin oxide (ITO)/Ag rear contacts. The current-voltage characteristics and quantum efficiency of these cells were measured.

3. Results and discussion

3.1. Film deposition

ZnO films were deposited at different temperatures with various ethanol to DEZ ratios. A small amount of water in the ethanol plays an important role in the deposition process. Water is the most common impurity in ethanol. After water was removed from the ethanol by slowly distilling from magnesium, the films grew very slowly and were easily peeled from the substrate. When small amounts of water were introduced into the reactor, the film adhered strongly on the substrate. If the ethanol to water mole ratio was kept above 250, the film growth rates did not change significantly as the water concentration was varied. Undoped films with roughness suitable for solar cells were deposited at 435 °C with an ethanol to water mole ratio of about 250. Higher water concentrations in the gas mixture (ethanol to water ratio below about 100) produce very smooth films. The dopant hexafluoropropene slightly increases the film growth rate and makes the film become smoother even at higher temperatures. Doped films with sufficient roughness for solar cells were obtained by first depositing undoped film for about 30 s on the substrate and then turning on the dopant, thereby minimizing the dopant influence on the initial stage of the film deposition processes. In addition to controlling the texture, this delayed doping minimizes the electrical resistance by confining the doping to the larger crystallites in the upper portions of the film, where the electrons have a higher mobility.

The film growth rates were obtained from samples deposited with thicknesses below 1500 Å by controlling the deposition time. Figure 2 shows that at 350 °C and a total gas flow of 12.0 l min⁻¹, the peak growth rate of ZnO for a fixed DEZ concentration first increases with increasing ethanol concentration in the gas mixture. However, higher ethanol concentrations decrease the growth rate slightly. When the DEZ concentration in the reactant

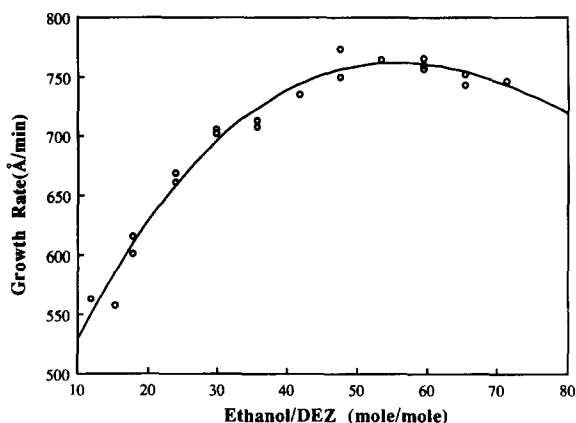


Fig. 2. Growth rate as a function of the concentration ratio of ethanol to DEZ. The deposition temperature is 350 °C and the DEZ concentration is 0.065%.

gas mixture is 0.065%, the highest growth rate is found for an ethanol to DEZ mole ratio of about 60. Figure 3 is a plot of peak growth rate *vs.* DEZ concentration for constant ethanol concentration of 5.9%. In the low DEZ concentration region, the growth rate depends linearly on DEZ concentration. As more DEZ is introduced into the reactor, white “smoke” can be seen coming out of the reactor and the measured peak growth rate increases more slowly than linearly.

From Fig. 4 it can be seen that the growth rate increases with temperature much faster in the high temperature range than in the low temperature range. This temperature dependence of the growth rate observed in our experiments is different from that reported in the literature [9]. This difference may lie in the reactor geometry. It is also found that the films cover smaller areas

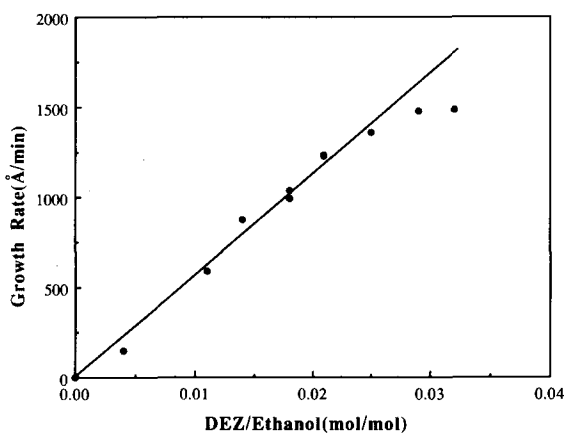


Fig. 3. Growth rate as a function of the concentration ratio of DEZ to ethanol. The deposition temperature is 350 °C and the ethanol concentration is 5.9%.

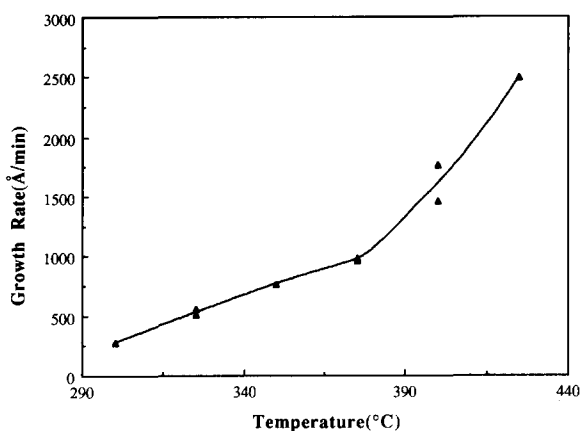


Fig. 4. Growth rate of ZnO film as a function of substrate temperature. The concentrations of DEZ and ethanol are 0.065% and 3.8%, respectively.

and become hazy as the deposition temperature increases. The haze results from the roughness of the film which produces more light scattering from the surface. Above 375 °C the roughness of the film increases very quickly and the ellipsometer becomes less reliable for the determination of film thickness; thus no thickness measurements are reported for temperatures above 425 °C.

3.2. Film structure and composition

The X-ray diffraction spectrum of a ZnO film deposited at 400 °C, shown in Fig. 5, shows that the films are crystalline. Only the (002) diffraction peak could be found; therefore the crystallites are highly oriented with their c-axes perpendicular to the plane of the substrate. At both higher and lower temperatures, the films are less oriented and other weaker diffraction peaks can be observed. The (112) peak appears on the spectra of films deposited at 325 °C but the (101) peak is not visible. However, the opposite situation is observed for films deposited at 425 °C for which the (112) peak disappears and the (101) can be observed. At 400 °C the dopant hexafluoropropene has no influence on the crystallite orientation and doped films are still highly c-axis oriented.

The films deposited below 350 °C showed no structure on the scanning electron micrographs (Fig. 6). At a deposition temperature of 400 °C, globular crystallites densely cover the whole substrate. At still higher temperatures the crystallites become larger and hexagonal with holes between crystallites, and the film appears to be less dense than bulk ZnO. The hexagonal crystallites clearly indicate that the film is oriented with c-axis perpendicular to the substrate, which is consistent with the information from X-ray diffraction. The electron micrographs of doped films were found to be the same as those for undoped films deposited at 400 °C, in agreement with the X-ray data. At higher deposition temperatures, however, the doped films are less rough than the undoped films.

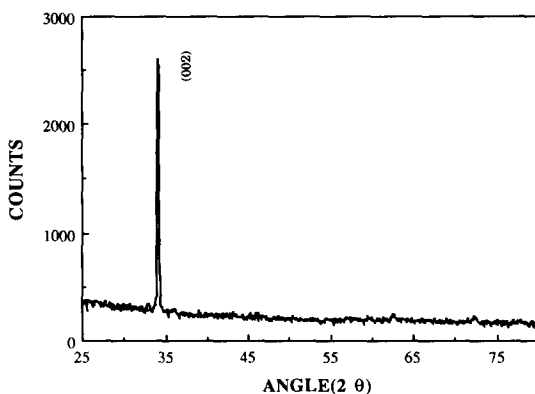


Fig. 5. X-ray diffraction spectrum of ZnO film deposited at 400 °C on soda lime glass.

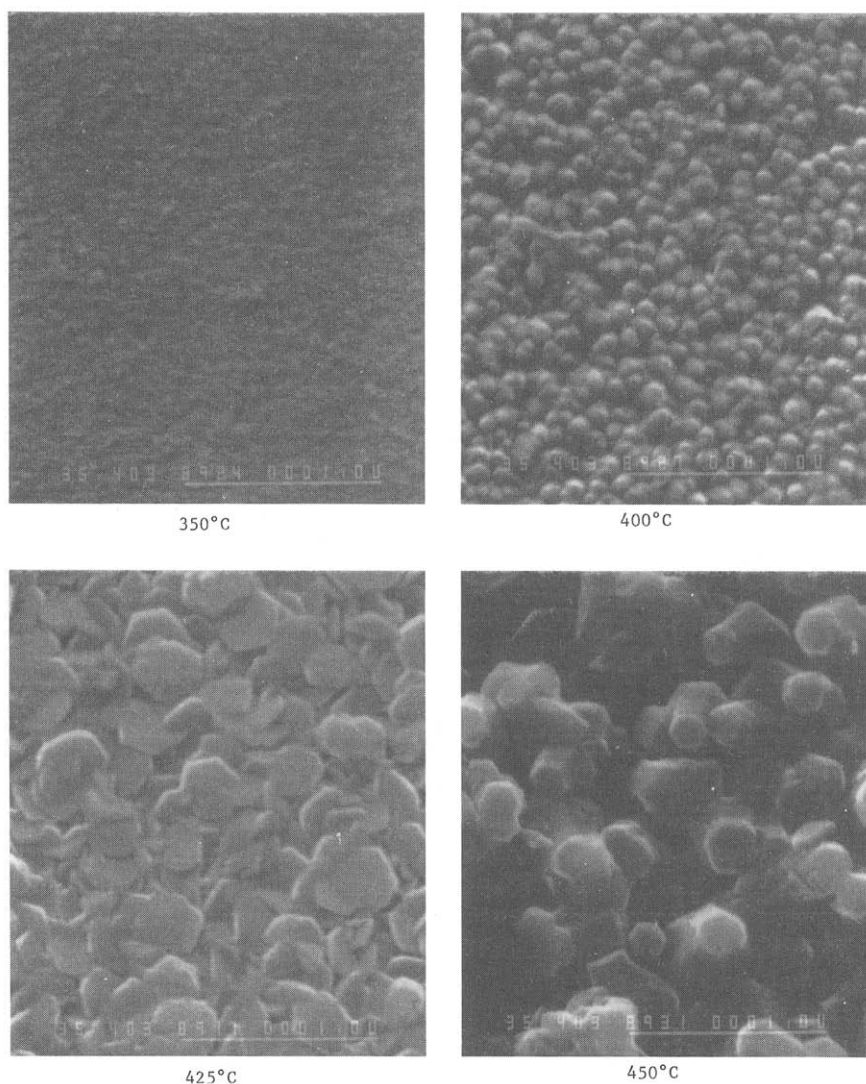


Fig. 6. SEM micrographs of ZnO films deposited at different temperatures.

The crystallite grain heights were determined from the widths of the (002) X-ray line. These grain heights, plotted in Fig. 7, increase with increasing deposition temperature. Grain widths were estimated by counting grains on the micrographs. These estimates, also plotted on Fig. 7, agree qualitatively with the X-ray data in showing an increase in size with increasing temperature. At temperatures above 400 °C, the (X-ray) grain heights are smaller than the (SEM) grain widths, in agreement with the flat platelet shapes seen in the micrographs.

The fluorine content was found to vary from 0.1 to 1.0 at.% for highly conductive ZnO films. The fluorine concentration in a film is inhomogeneous

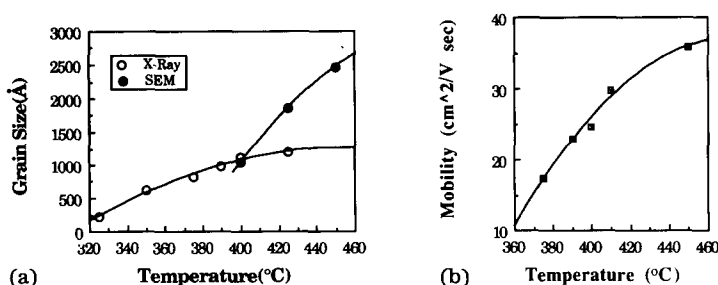


Fig. 7. (a) Grain size of polycrystalline ZnO films as a function of deposition temperature. (b) Electron mobility in ZnO:F films as a function of deposition temperature.

TABLE 1

Composition and properties of ZnO films deposited at various temperatures. The DEZ and ethanol concentrations are 0.065% and 3.8% respectively, and the dopant gas (hexafluoropropene) concentration is 0.14%

Sample	T_d (°C)	Fluorine content (at.%)	Electron conductivity ($\Omega^{-1} \text{ cm}^{-1}$)	Electron concentration (cm^{-3})	Electron mobility ($\text{cm}^2 \text{ V}^{-1} \text{ s}^{-1}$)	Doping efficiency (%)
A	375	0.62	0.93×10^3	3.36×10^{20}	17	65
B	390	0.58	1.35×10^3	3.67×10^{20}	23	76
C	400	0.48	1.53×10^3	3.85×10^{20}	25	97
D	410	0.42	1.41×10^3	2.96×10^{20}	30	85
E	450	0.25	1.15×10^3	2.00×10^{20}	36	96

along the gas flow direction, which is a typical feature of CVD processes in which gas phase reactions alter the composition of the gas phase along the flow direction. Usually the position of highest growth rate is not the same as the position of highest fluorine content. The fluorine concentrations of films deposited at different temperatures are listed in Table 1. Those samples were selected from the most conductive parts on the substrate. At constant dopant gas flow, more fluorine usually can be incorporated into the film as the temperature increases. However, higher temperatures lead to a more rapid increase in the film deposition rate than in the fluorine incorporation rate, and thus to a lower fluorine concentration in the film.

The electron microprobe is not sensitive enough to determine carbon. X-ray photospectrometry detected carbon contamination on the film surface but only a very small amount of carbon (less than 1 at.%) could be detected after the surface layers were sputtered away. No other impurities were detected. Some hydrogen may be present in the films, but analytical tools for its quantitative estimation were not available.

3.3. Optical properties

The free electrons in the doped ZnO films modify some of their optical properties. In the infrared range, the doped films behave like metals, having

high reflectance and low transmittance (Fig. 8(a)). In the visible range, however, the films are highly transparent and their reflectance spectra look like those of dielectrics. The crossover between these two types of behavior is the so-called plasma wavelength which moves to shorter wavelengths as the free electron density in the film increases. Figures 8(a) and 8(b) show the total reflectance, transmittance and absorption for a doped film deposited at 435 °C. Figure 8(c) shows diffuse transmission curves at a number of temperatures. The diffuse transmission increases with increasing substrate temperature, which shows the increasing roughness of the films deposited at higher temperatures. The intensity of diffuse components increases at shorter wavelengths. The absorption in the visible range was averaged with weighting factors of the solar spectrum and a-Si solar cell efficiency. The total absorption was found to be about 3% for a film thickness of 0.78 μm and a sheet resistance of 5.2 Ω/\square . The visible transmission, averaged over these same weighting factors, is 87%.

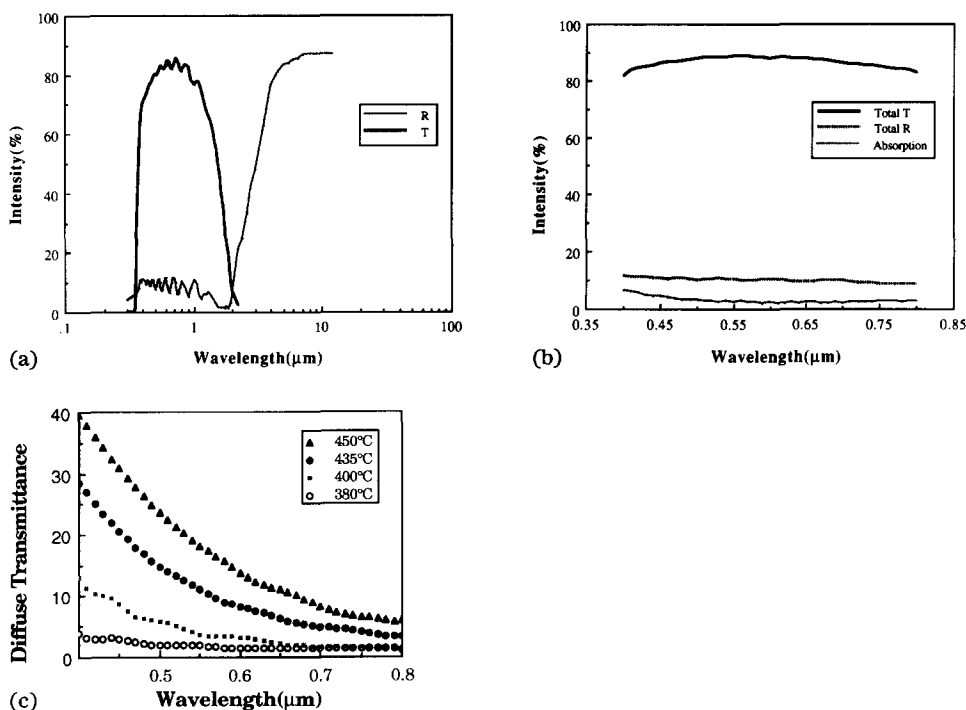


Fig. 8. Reflectance, transmittance and absorbance of a doped ZnO film deposited at 435 °C. The concentrations of DEZ, ethanol and hexafluoropropene are 0.065%, 3.8% and 0.14%, respectively. (a) Total transmission and reflection of a film on soda lime glass in the infrared and visible. (b) Total reflectance, transmittance and absorption determined by covering the film surface with a thin layer of liquid with refractive index 1.74 and a glass sheet, to reduce the influence of the rough film surface. (c) Diffuse transmittance in the visible range, for films deposited at various temperatures.

3.4. Electrical characterization

The film conductivity was determined from the measured sheet resistance and thickness. Fluorine was found to be an n-type dopant for ZnO, which increases the free electron concentration and film conductivity. A fluorine concentration of about 0.5 at.% gives the highest conductivity, for films deposited at 400 °C (Fig. 9). Such an optimally doped film has about 1% of its oxide ions replaced by fluoride ions.

The measured Hall coefficient can be used to calculate the free electron density of the film. As more fluorine is incorporated into the film the electron density first increases and then decreases, as shown in Fig. 10. Comparing Figs. 9 and 10, it is obvious that the highest conductivity and highest free electron density are both obtained for films with the same fluorine content. The electron mobility μ_H can be determined from the Hall coefficient R_H and the conductivity σ following a simple formula $\mu_H = R_H \sigma$. Whereas mobilities in lightly doped single crystal ZnO are typically around $180 \text{ cm}^2 \text{ V}^{-1} \text{ s}^{-1}$

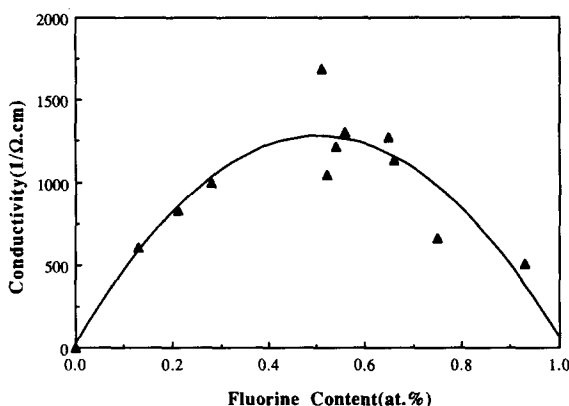


Fig. 9. Conductivity of doped ZnO films deposited at 400 °C as a function of fluorine content.

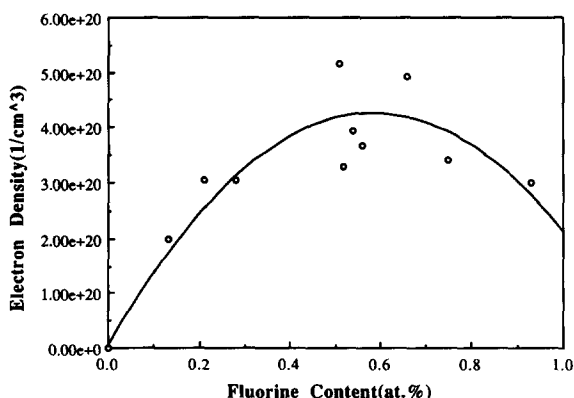


Fig. 10. Free electron density of doped ZnO films, determined from the measured Hall coefficients. The deposition temperature is 400 °C.

[10], the mobilities for the polycrystalline fluorine-doped ZnO films varied from 10–40 $\text{cm}^2 \text{V}^{-1} \text{s}^{-1}$. These lower values may be expected for polycrystalline films because the carriers undergo scattering by the grain boundaries. High fluorine concentrations will also increase the scattering and therefore decrease the mobilities. Films doped with boron, aluminum or indium [3, 4] show still lower mobilities (typically up to 20 $\text{cm}^2 \text{V}^{-1} \text{s}^{-1}$) than these fluorine-doped films. These results confirm the theoretical argument, given in the introduction, that fluorine should be a superior dopant for ZnO.

Figure 11 shows mobility as a function of fluorine concentration for films deposited at 400 °C. The temperature dependence of the film conductivity, electron density and mobility are also listed in Table 1. The mobility increases with deposition temperature (Fig. 7(b)), mainly because there are fewer grain boundaries in the films deposited at higher temperatures.

The deposition temperature can strongly influence both the reactivity of the dopant gas and the movement of dopant atoms to the positions in which they are electrically active. The doping efficiency η_{DE} , defined as the ratio of the free electron concentration to the fluorine atom concentration, gives the fraction of the fluorine atoms that are electrically active in the film. It can be calculated from the electron concentration, the fluorine percentage and the ZnO density, which is taken to be the same as the bulk density 5.606 g cm^{-3} . The doping efficiency increases as the temperature increases (Table 1). At deposition temperatures below 350 °C, although some fluorine atoms can still be introduced into the film, they are not active as donors. Perhaps they do not occupy the correct positions (oxygen sites) inside the ZnO crystals and so they do not contribute free electrons to the film and increase film conductivity. These inactive fluorine atoms may introduce new states in the band gap and may decrease the film conductivity by providing more scattering centers.

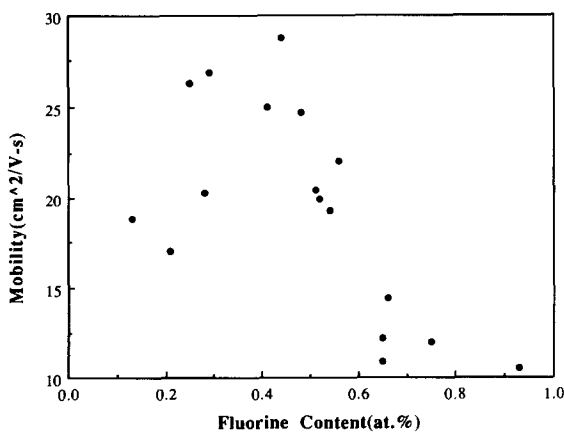


Fig. 11. Electron mobility as a function of fluorine content for doped ZnO films deposited at 400 °C.

TABLE 2

Sheet resistance, quantum efficiency, fill factor (FF) and open circuit voltage V_{oc} of solar cells made from ZnO:F films. The concentrations of DEZ and ethanol are 0.065% and 3.8% respectively, and the dopant concentration was varied

Sample	Temp. (°C)	Dopant (mole %)	Resistance (Ω/\square)	Quantum efficiency at -3 V			FF (%)	V_{oc} (V)
				400 nm	700 nm	peak value		
1644	443	0.17	11	0.64	0.50	0.87	45	0.727
1650	422	0.17	11	0.67	0.57	0.89	46	0.748
1651	426	0.17	4	0.67	0.60	0.90	50.1	0.760
1653	456	0.17	7	0.66	0.61	0.87	50.3	0.784
1654	469	0.13	7	0.74	0.65	0.86	48	0.71
1645	443	0.13	17	0.66	0.535	0.892	50	0.730
Control			20	0.66	0.47	0.84	60.4	0.846

3.5. Solar cell characterization

A-Si-based solar cells typically have a relatively poor quantum efficiency in the red region of the visible spectrum due to the low absorption coefficient of a-Si:H in this region. In order to increase the absorption of red light in the intrinsic a-Si:H layer, rough ZnO films can be used to scatter light into the silicon at a distribution of angles. Another effect of the rough surface is to provide an optical transition layer between the silicon and ZnO, thereby reducing reflection losses by letting the photons experience a gradual change in refractive index from ZnO to a-Si:H. The optical constants of fluorine-doped ZnO are very similar to those of fluorine-doped SnO_2 . Light-trapping in a-Si solar cells based on rough SnO_2 , was optimum for diffuse transmission from about 5 to about 10% for red light [11]. The rough ZnO films grown at 435–450 °C show this optimum amount of diffuse transmission (see Fig. 8(c)), and therefore should be ideal substrates for solar cells.

Textured, fluorine-doped ZnO with different resistance, roughness and absorption on various parts of the substrates were used to prepare “standard” p a-SiC:H/i a-Si:H/n a-Si:H devices with ITO/Ag rear contacts. The very high quantum efficiency (up to 65%, as seen in Table 2) at 700 nm suggests that the textured ZnO films produce sufficient scattering at long wavelengths to trap light efficiently. The high peak quantum efficiencies indicate that the films have low parasitic absorption, in agreement with the optical measurements. The devices were found to have lower open circuit voltages and fill factors than comparable controls. The poor fill factors and open circuit voltages may simply reflect the need to optimize the p-layer thickness for these substrates, or may arise from contamination on the film surface.

4. Conclusions

We prepared fluorine-doped ZnO films by atmospheric pressure chemical vapor deposition from diethylzinc, ethanol, water and hexafluoropropene at

various temperatures. X-ray diffraction and SEM revealed that the films are highly oriented with their c-axes perpendicular to the substrate. The grain size was found to increase rapidly with increasing deposition temperature and with decreasing water and hexafluoropropene concentration. Films containing 0.5 at.% fluorine and deposited at temperatures above 400 °C give the highest conductivity, mobility and free electron density. The doped films have high infrared reflectance, high visible transmittance and low absorption in the visible. Rough films were obtained by depositing at higher temperatures (above 400 °C) and by introducing a small amount of water vapor into the reactor. Solar cells made from rough ZnO:F films have very high quantum efficiencies (up to 90%). We conclude that CVD at atmospheric pressure is able to produce highly conductive and transparent ZnO films suitable for efficient transparent electrodes in solar cells.

Acknowledgments

This work was supported by the Solar Energy Research Institute under Subcontract XX-8-18148-1. Instruments of Harvard Materials Research Laboratory, supported by the National Science Foundation, were also used. The Watkins-Johnson Company donated the gas dispersion nozzle. We thank Dr. Anthony Catalano of Solarex Inc. for preparing the solar cells and measuring the cell parameters. Dr. Catalano also suggested the use of the high-index liquid for estimating film absorption.

References

- 1 Z. C. Jin, I. Hamberg and C. G. Granqvist, *J. Appl. Phys.*, **64** (1988) 5117.
- 2 R. G. Gordon and J. Hu, Final Technical Report, SERI Subcontract XX-8-18148-1 (1989).
- 3 P. S. Vijayakumar *et al.*, U.S. Patent 4 751 149 (1988).
- 4 S. N. Qiu, C. X. Qiu and I. Shih, *Solar Energy Mater.*, **15** (1987) 261.
- 5 T. Minami, H. Nanto and S. Takata, *Jpn. J. Appl. Phys.*, **24** (1985) L605.
- 6 C. K. Lau, S. K. Tiku and K. M. Lakin, *J. Electrochem. Soc.*, **127** (1980) 1843.
- 7 F. T. J. Smith, *Appl. Phys. Lett.*, **43** (1983) 1108.
- 8 R. G. Gordon, unpublished results.
- 9 S. Oda, H. Tokunaga, N. Kitajima, J. Hanna, I. Shimizu and H. Kokado, *Jpn. J. Appl. Phys.*, **24** (1985) 1607.
- 10 D. R. Lide, *Handbook of Chemistry and Physics*, 71st Edition, CRC Press.
- 11 R. G. Gordon, J. Proscia, F. B. Ellis, Jr. and A. E. Delahoy, *Solar Energy Mater.*, **18** (1989) 263.